MRS Communications (2018), *8*, 241–247
© Materials Research Society, 2018
doi:10.1557/mrc.2018.54

MRS Communications

Research Letter

Biomimetic protein-harpooning surfaces

G. M. L. Messina, Laboratory for Molecular Surfaces and Nanotechnology (LAMSUN), Department of Chemical Sciences, University of Catania and CSGI, Viale A. Doria 6, Catania 95125, Italy
C. Bonaccorso and **A. Rapisarda,** Department of Chemical Sciences, University of Catania, Viale A. Doria 6, Catania 95125, Italy
B. Castroflorio, Laboratory for Molecular Surfaces and Nanotechnology (LAMSUN), Department of Chemical Sciences, University of Catania and CSGI, Viale A. Doria 6, Catania 95125, Italy
D. Sciotto, Department of Chemical Sciences, University of Catania, Viale A. Doria 6, Catania 95125, Italy
G. Marletta, Laboratory for Molecular Surfaces and Nanotechnology (LAMSUN), Department of Chemical Sciences, University of Catania and CSGI, Viale A. Doria 6, Catania 95125, Italy

Address all correspondence to G. M. L. Messina at **grmessi@unict.it** and C. Bonaccorso at **bonaccorsoc@gmail.com**

(Received 17 January 2018; accepted 26 March 2018)

Abstract

Properly driving protein interactions with solid surfaces play a very important role in many natural processes, stimulating a great interest for the design of new biomaterials and medical devices. Despite the progress in this field, many further upgrades have to be achieved to better exploit the protein driving, in terms of control of amounts and conformation of the adsorbing proteins. In this paper, new biocompatible amino acid–calix[4]crown-5 bilayers were built as nano-templating surfaces, hosting a controlled number of anchoring sites, able to immobilize proteins in well-defined quantity, and the evaluated footprint data support the idea of oriented protein on analyzed substrates. The efficiency of the setup was tested for the particular case of antibacterial lysozyme adsorption on biocompatible surfaces.

Introduction

Specific anchoring of proteins at solid/liquid interface plays an important role in various biologic processes, including the development of tissue engineering substrates, biomolecule recognition, antibacterial surfaces, etc.[1–7]

Surface-bound host–guest assemblies, consisting of amino acid–calix[4]crown-5 (calixarenes) bilayers, have been shown to be able to drive the protein organization and dynamics at interfaces, including their packing, orientation state, native and denatured state, aggregation propensity, and, in turn, their global biologic response.[8–13]

The calixarenes, thanks to their synthetic accessibility and versatility, have gained attention for a wide range of applications in chemical, analytical, and engineering materials fields.[14, 15] Recently, we have exploited calixarenes for molecular recognition and self-assembly,[16, 17] reversible supramolecular hydrogels,[18] and as catalysts.[19]

In this paper, we propose a new concept of nano-structured surfaces able to "harpoon" biomolecules, including simple amino acids and a model protein, in a controlled way, based on the templating properties of a new calix[4]arene-crown-5 (TCC5), which is covalently anchored onto gold surfaces, forming uniform monolayers.

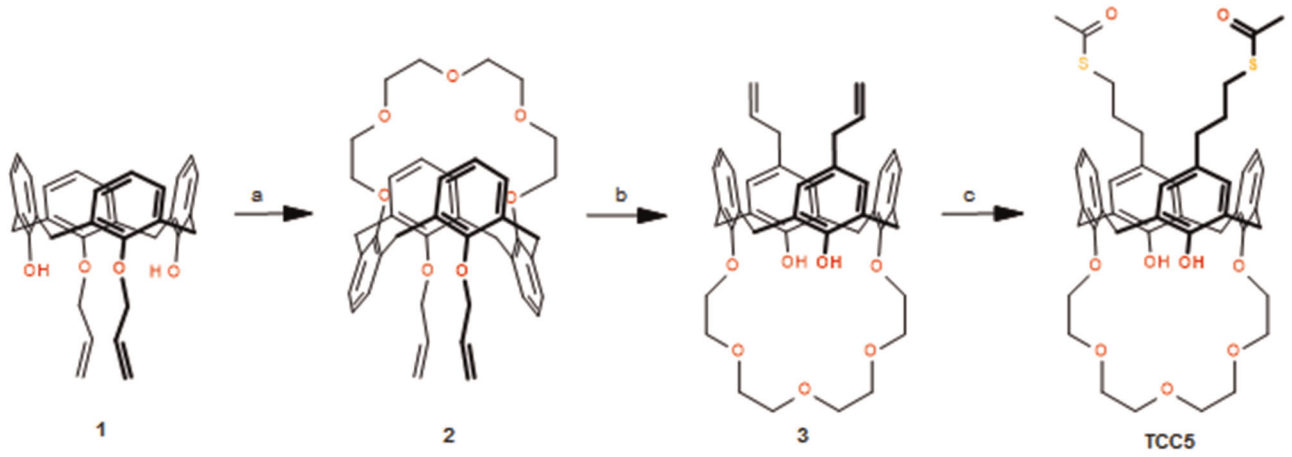
The formation of the calix monolayer, the subsequent amino acids interaction, as well as the protein uptake, both on the mono (TCC5) and bilayers (TCC5-amino acid functionalized), were analyzed in situ by means of quartz crystal microbalance with dissipation monitoring (QCM-D), in order to quantitatively determine the surface coverage, the specific adsorption kinetics of each component and the viscoelastic behavior of the adsorbed species. Different amino acids, i.e., polar (serine), non-polar (alanine), acidic (aspartic acid), and basic (lysine), have been used to assess the effect of their structural features on the interaction with the hosting calix layer and the lysozyme, respectively. The experimental results have been analyzed in the framework of the random sequential adsorption (RSA) model.[20]

The TCC5 was designed to contain the crown-5 moiety as the hydrophilic head and two alkyl chains with terminal thioacetate groups as the hydrophobic tail to allow a stable linkage on the gold surface. The synthetic procedure to TCC5 is depicted in Scheme 1.

The use of acetyl-protected thiols, which will be deprotected in situ just before or during the organic film formation, provides an excellent way to alleviate the problems of isolating and using thiols, to minimize unwanted oxidation, disulfide formation, or polymerization on the gold surface of the QCM-D sensor (see Supplementary material for further details).[21, 22] To the best of our knowledge, this procedure has never been employed for the anchoring of calixarenes on gold.

The formation of a self-assembled monolayer of TCC5 on the gold surface occurs in a quite long time [about 18 h, see Fig. 1(a)], in agreement with known data on thiols binding to Au surfaces.[23] The anchoring process was studied by using in situ QCM-D measurements, which give information about

https://doi.org/10.1557/mrc.2018.54 Published online by Cambridge University Press



Scheme 1. Synthesis of calix[4]crown-5 (TCC5): (a) Cs_2CO_3, tetraethylene glycol ditosylate, CH_3CN, reflux; (b) dimethylaniline, reflux; (c) 2,2′-azobis (2-methylpropionitrile) (AIBN), thioacetic acid, toluene, reflux.

mass uptake, derived from the shift of the sensor resonance frequency (Δf), and viscoelastic properties of the adsorbed molecules, in turn, figured out from the changes in dissipation value (ΔD). The measurement chamber had a volume of 80 µL and the simultaneous measurements of frequency (f) and energy dissipation (D) were performed for the fundamental resonance frequency ($n = 1$, i.e., $f \sim 5$ MHz) and the several overtones roughly corresponding to slightly different sampling depth[24] ($n = 3$, 5, 7, 9, 11, 13 corresponding to $f \sim 15$, ~25, ~35, ~45, ~55, and ~65 MHz, respectively).

In particular, a relatively high ratio (i.e., $|\Delta f/\Delta D| \geq 20$ Table I) allows considering the adsorbed mass as a rigid layer, enabling to calculate the mass uptake by applying Sauerbrey equation[25]:

$$\Delta m = -(C/n) \cdot \Delta f,$$

where Δf is the decrease in resonant frequency, Δm is the mass uptake at the sensor surface, C is a constant depending on the intrinsic properties of quartz slab (in our case $C = 17.7$ ng/cm^2 Hz^{-1} at $f = 5$ MHz), and n ($= 1, 3, \ldots$) is the overtone number. Each harmonic of the resonating frequency penetrates to a different distance from the sensor surface. Higher harmonics probe relatively close to the surface of the sensor, whereas lower harmonics extend beyond the adsorbed layer into the bulk solution. The resolution in f and D is, respectively, ±0.1 Hz and 1×10^{-7}.

The stability of the bound TCC5 molecules, after reaching the first apparent saturation state, was verified in the QCM-D measurement chamber by in situ flushing step with pure ethanol, which induced the desorption of a small percentage of unbound TCC5 molecules, roughly involving the 11% of the initially adsorbed molecules. This rules out the occurrence of

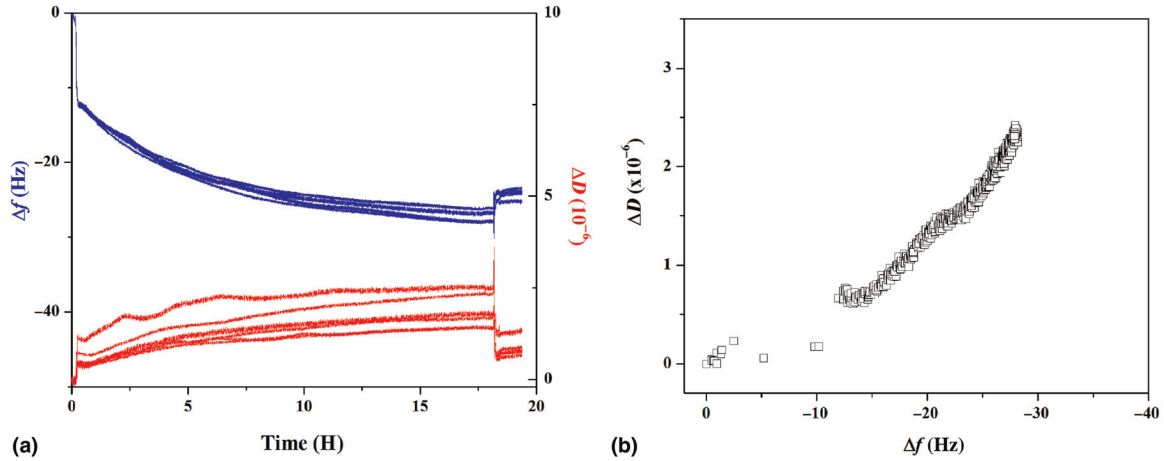


Figure 1. (a) Frequency plot and dissipation plot for the TCC5–Au substrate interaction; (b) D–f plot showing the viscoelasticity versus adsorbed mass. Overtones from $n = 1$ to $n = 13$ are shown.

https://doi.org/10.1557/mrc.2018.54 Published online by Cambridge University Press

Table I. Adsorption of TCC5 on Au and amino acid on TCC5 monolayer.

	pI aa	Δf (Hz)	ΔD (10^{-6})	Adsorbed mass (ng/cm^2)	Molecules/cm^2
Calix		−22.9 ± 0.5	0.9 ± 0.3	406.0 ± 8.8	$3.0 \times 10^{14} \pm 0.1 \times 10^{14}$
Alanine	6.11	−6.1 ± 0.6	0.0 ± 0.1	107.4 ± 10.6	$7.2 \times 10^{14} \pm 0.7 \times 10^{14}$
Aspartic acid	2.85	−8.0 ± 0.8	0.1 ± 0.1	142.1 ± 14.6	$4.9 \times 10^{14} \pm 0.5 \times 10^{14}$
Lysine	9.60	−6.7 ± 0.5	0.1 ± 0.3	118.1 ± 8.8	$4.8 \times 10^{14} \pm 0.4 \times 10^{14}$
Serine	5.68	−9.3 ± 0.6	0.1 ± 0.2	163.9 ± 10.6	$9.4 \times 10^{14} \pm 0.6 \times 10^{14}$

a multilayer adsorption, as we expect that only the strong thiol–Au bonds (about 89% in the present case) resisted the flushing treatment with ethanol, thus suggesting the formation of a compact and strongly bound TCC5 monolayer on the Au substrate.

Indeed, Fig. 1 shows that all the recorded overtones for the adsorbed monolayer are very close each other, confirming the rigidity of the adsorbed calix films, also confirmed by the decrease of the dissipation from about 1.8×10^{-6} to 0.9×10^{-6}, following the washing step.

The frequency and dissipation data for the adsorbed film at the steady state have been used to estimate the actual number of TCC5-bound molecules and, in turn, the coverage percentage. As mentioned above, the Sauerbrey equation[25] could be used, owing to the low dissipation value (ΔD) for the bound molecules. The measured mass corresponds to about $3.0 \times 10^{14} \pm 0.1 \times 10^{14}$ TCC5 molecules/cm^2, i.e., a compact monolayer, in good agreement with literature data for very similar calix [4]crown-5.[26] Additional information can be extracted from the *D–f* plots [Fig. 1(b)], which shows the correlation between dissipation (ΔD) and frequency (Δf) values, providing the kinetic regime information in terms of density and slope of the *D–f*, the faster the kinetics, the more disperse the measured points and the steeper the slope of the experimental curve. In our case, the *D–f* plot shows that the anchored TCC5 molecules behave as a weakly viscoelastic monolayer.

The anchored TCC5 monolayers have been used as substrates to adsorb the four model amino acids, i.e., lysine, aspartic acid, serine, and alanine. In Table I, the pI of each amino acid used in this work were reported; at pH value used for experiment 7.4, alanine and serine have a weak charge, whereas aspartic acid and lysine have a net negative and positive charge, respectively. Figure 2(a) shows that the amino acids mass uptake, at pH = 7.4 and ionic strength 0.2 M, occurs with the same kinetic law and the mostly rigid behavior for all the tested amino acids [Fig. 2(b) and Table I], in spite of the striking differences among them.

It is to stress that, all the adsorbed amino acids resist the washing step after reaching the steady state, suggesting a firm immobilization on the calix monolayer. In our case for all investigated amino acids adsorbed on TCC5 monolayer, the adlayers behave as stiff films, and by applying Sauerbrey equation, it is possible to calculate the adsorbed mass that can be used to obtain an "effective" number of immobilized molecules for each amino acid. In this case, as all frequency shifts are very close, only the third overtone is shown for each amino acid, due to its higher sampling depth, ensuring that the whole calix–amino acid bilayer is taken into account.

Table I shows that the number of the adsorbed alanine and serine molecules, i.e., the low molecular weight species, is higher than the estimated number of anchoring calix molecules, respectively, by a factor of 2 for alanine and 3 for serine. On the other hand, aspartic acid (negatively charged) and lysine (positively charged) are adsorbed in a similar amount, closer to the number of anchored calix molecules, so that the interaction between calix and amino acids does not seem strictly electrostatic, but it must be driven by additional strong intermolecular forces. Anyhow, the adsorption kinetic [see *D–f* plots in Fig. 2(b)] is of the first order and the kinetic regimes for the various amino acid/calix couples show the same trend.

The TCC5 monolayers and the TCC5–amino acid bilayers were further used as substrates to study the adsorption conditions of lysozyme, as model protein [see Figs. 2(c) and 2(d)], comparing their behavior with that of a reference clean gold substrate, in order to evaluate the role of the unspecific interactions.

The dissipation for the protein adsorbed onto the various substrates is always lower than 1.0×10^{-6}, again enabling the use of Sauerbrey equation to calculate the adsorbed mass from the measured frequency shift. More, in particular, it can be seen that:

(i) The lysozyme adsorption onto bare gold exhibits a peculiar decreasing trend, diagnostic of extensive structural rearrangements of the adsorbed protein. As suggested by Rabe et al.,[27] this adsorption mechanism, in this case, can be represented by a three-state model in which the last slower transition state involves some conformational arrangement;

(ii) The adsorbed lysozyme mass on both the TCC5 monolayer and the TCC5–amino acid bilayers is lower than for reference gold substrate, roughly by a factor of 2.

(iii) Lysozyme is sharply adsorbed onto the TCC5–amino acid bilayers, reaching immediately a stable saturation level, while a slow adsorption drift is found for bare TCC5 monolayers.

https://doi.org/10.1557/mrc.2018.54 Published online by Cambridge University Press

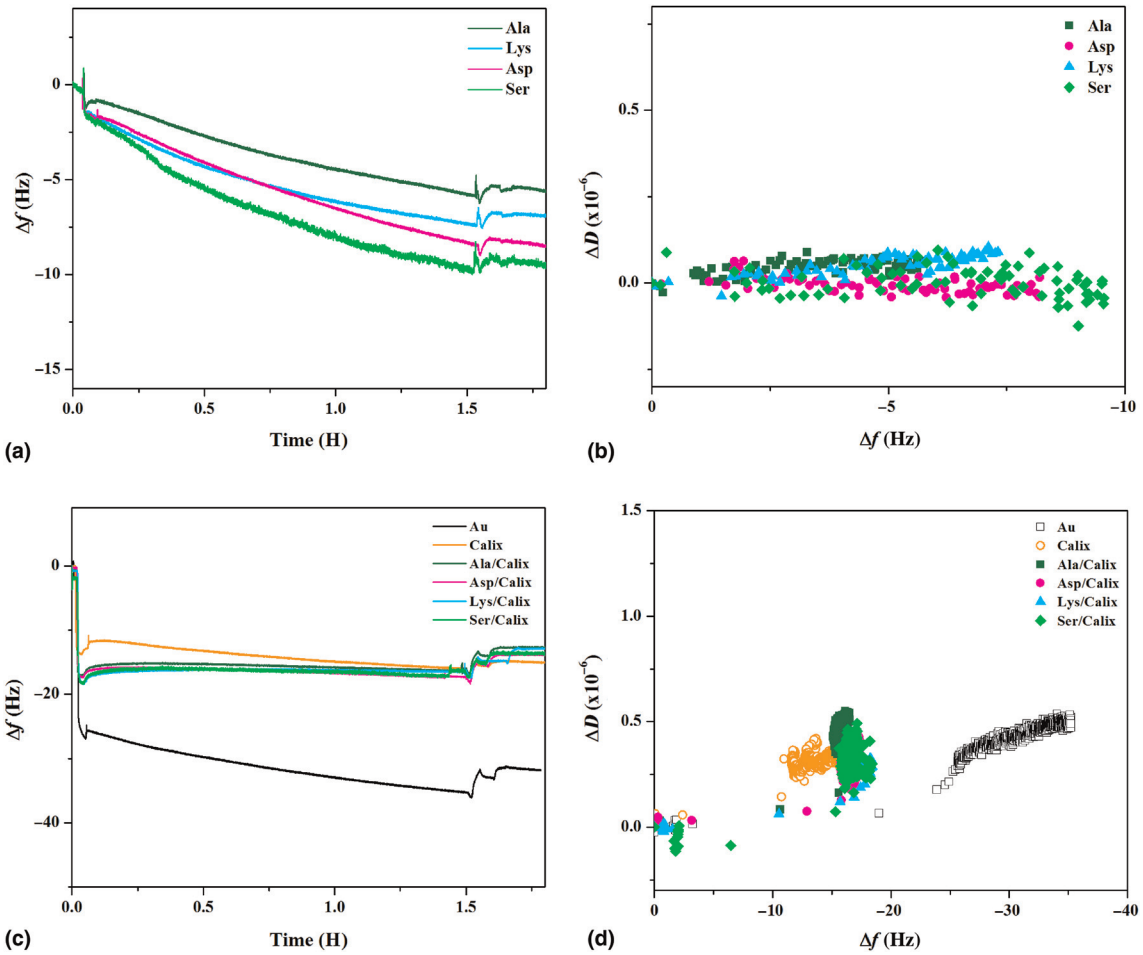


Figure 2. (a) Frequency plot for the amino acid–TCC5 interaction; (b) *D*–*f* plot showing the adsorbed molecule viscoelasticity and interaction kinetics; (c) frequency plot for the lysozyme on TCC5–amino acid bilayers adsorption; (d) *D*–*f* plot showing the kinetics of interaction of lysozyme with the various substrates. Only the third overtone is shown, due to its higher sampling depth.

(iv) Moreover, the adsorbed mass of lysozyme is very similar for all the bilayer substrates, in spite of the fact that alanine and serine are adsorbed in higher quantity, and in turn is very similar to the final adsorbed mass on TCC5 monolayers.

The QCM-D traces indicate that, at a variance of the not saturating adsorption trend observed for bare gold, a slow adsorption is found for TCC5 monolayer (suggesting minor conformation rearrangements), a quick saturation occurs for all the bilayers, diagnostic of the sharp and irreversible immobilization of the adsorbed lysozyme. However, it is noteworthy that the steady-state amount of immobilized protein is similar for TCC5 monolayer and all the bilayers, and is lower by a factor of 2 than to gold, as shown in Table II. These data allow also estimating the number of lysozyme molecules adsorbed on the various substrates.

We suggest that the non-saturating adsorption of lysozyme on the bare gold substrate can be attributed to the non-specific interactions, with a continuously growing amount of adsorbed protein, due to the dynamic reorganization of the adsorbed molecules, congruent with a multilayer formation. Indeed, the related average apparent footprint for lysozyme on gold is about 500.00 Å^2 for the $2.0 \times 10^{13} \pm 0.08 \times 10^{13}$ adsorbed molecules. This area is remarkably smaller than both the theoretical end-on footprint (about 909.00 Å^2) and side-on footprint (about 1350.00 Å^2), derived from the native state size (4.5 nm × 3.0 nm × 3.0 nm),[28] supporting our suggestion that actually a protein bilayer is adsorbed onto the bare gold substrate.

Table II also shows that the overall amount of lysozyme (i.e., about 50% or less than the quantity measured for the gold substrate) is quickly adsorbed onto both TCC5 monolayer and TCC5–amino acid bilayers. This suggests that, in those cases, a protein monolayer is adsorbed on the surfaces. Indeed, the footprint of lysozyme adsorbed onto bare TCC5 monolayer (i.e., 909.00 Å^2) is close to the expected area of a stable monolayer of oriented protein in an almost perpendicular end-on

https://doi.org/10.1557/mrc.2018.54 Published online by Cambridge University Press

Table II. Lysozyme adsorption on TCC5 and TCC5–amino acid bilayers.

Lysozyme on	Adsorbed mass (ng/cm^2)	Molecules/cm^2	Average lysozyme footprint (Å^2)	S (cm^2/s)	k_c (cm/s)
Au	541.7 ± 22.5	$2.0 \times 10^{13} \pm 0.1 \times 10^{13}$	500	3.6×10^{-6}	6.3×10^{-4}
TCC5	297.6 ± 14.0	$1.1 \times 10^{13} \pm 0.1 \times 10^{13}$	909	1.5×10^{-6}	3.6×10^{-4}
Ala/TCC5	241.3 ± 4.6	$8.9 \times 10^{12} \pm 0.0 \times 10^{13}$	1123	2.3×10^{-6}	4.7×10^{-4}
Asp/TCC5	253.6 ± 8.5	$9.4 \times 10^{12} \pm 0.0 \times 10^{13}$	1064	1.9×10^{-6}	4.1×10^{-4}
Lys/TCC5	228.4 ± 3.2	$8.4 \times 10^{12} \pm 0.0 \times 10^{13}$	1190	2.1×10^{-6}	4.5×10^{-4}
Ser/TCC5	240.3 ± 8.3	$8.9 \times 10^{12} \pm 0.0 \times 10^{13}$	1123	2.1×10^{-6}	4.4×10^{-4}

configuration. At a variance of this, the footprints calculated from the adsorption of lysozyme onto amino acid/TCC5 bilayers is ranging between 1060 and 1190 Å^2, i.e., in good agreement with the hypothesis of a monolayer of slightly tilted end-on proteins.[29]

The above experimental data may be used to discuss the kinetics law of the adsorption processes for the various substrates. Figure 3(a) shows the lysozyme mass uptake onto Au substrates, TCC5 monolayer, and TCC5–amino acid bilayers.

As mentioned above, the adsorption onto bare gold does not reach the steady state, while the TCC5 monolayer and TCC5–amino acid bilayers quickly reach saturation. The unspecific adsorption on gold can be rationalized in terms of the three-state model, involving a fast initial unspecific random adsorption on the unstructured surface, followed by conformational reorganization, likely driven by protein–protein interactions, which yields a reversible adsorption state, finally leading to the third final relaxed and irreversibly adsorbed states, following slow conformational rearrangements.[27]

The lysozyme adsorption onto bare TCC5 monolayer and bilayers can be discussed in terms of the well-known "roll-over" mechanism, demonstrated for lysozyme by Wertz and Santore.[12] This mechanism involves the quick protein adsorption in end-on conformation, yielding a very stable monolayer onto the bare TCC5, while the adsorption onto the TCC5–amino acid bilayers seems to imply a variable degree of tilting of the initially end-on molecules, according to the specific TCC5–amino acid couple constrains.

To unravel the above-mentioned fast adsorption saturation process, we have focused on the analysis of the QCM-D data at very short times. Figure 3(b) reports the adsorption curves for the first minutes, showing that a very fast step (limited to about 1 min), involving the transport of the protein from the solution bulk to the surfaces, saturates the lysozyme adsorption onto TCC5 and TCC5–amino acid bilayers.

The RSA analysis provides the apparent diffusion coefficient S and the average mass transfer rate constant (k_c) characteristics for each process.

The apparent diffusion coefficient (S) can be calculated from the slope of the diffusion-controlled step, by using the

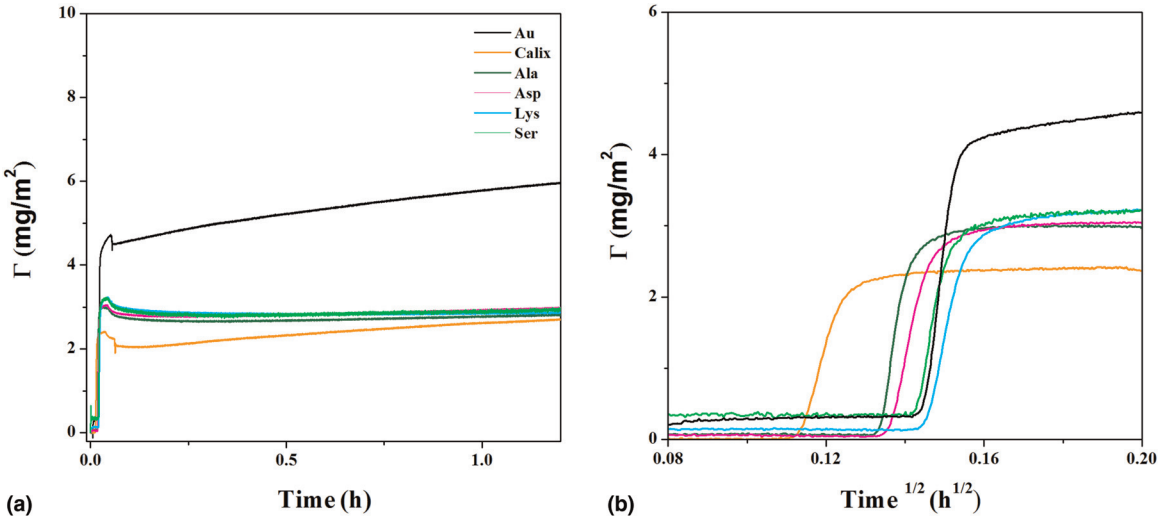


Figure 3. (a) Adsorption kinetics measured for lysozyme onto gold, TCC5, and TCC5–amino acid bilayers, (b) adsorption kinetics of first few minutes.

https://doi.org/10.1557/mrc.2018.54 Published online by Cambridge University Press

following equation[20]:

$$\Gamma(t) = \frac{2}{\sqrt{\pi}} c_{\text{bulk}} \sqrt{St},$$

where Γ is the adsorbed mass and c is the bulk concentration.

The average mass transfer rate constant (k_c) describes the efficiency of the convection-driven protein mass transport/binding at the surfaces and can be derived from the following equation[30]:

$$k_c = C_f Q^{1/3} S^{1/3},$$

where S is the "apparent" diffusion coefficient previously calculated (phenomenologically describing the sticking efficiency of the protein on the calix–amino acid constructs), $Q = 2.5 \times 10^{-3}$ cm^3/s is the volumetric flow rate employed in the experiments and $C_f = 19.9$ cm$^{-4/3}$ is a geometry-dependent factor for the employed QCM-D cell. It is noteworthy that C_f is independent of the solution concentration, flow rate, and protein size or shape.

Table II resumes the parameters derived for all the analyzed substrates. The S values are of the order of 10^{-6} cm^2/s and turn out to be very similar for all the substrates, with the only exception of gold, which shows a value about two times higher than the ones of the TCC5 and TCC5–amino acid substrates. This confirms that the initial protein–calix and protein–amino acid/calix substrates are not influenced by the charge of the amino acids.

On the other hand, the k_c values for the bare TCC5 are very close to the k_c values obtained for all the bilayers, confirming that the number of immobilized lysozyme molecules does not depend upon the number of amino acid molecules, which is indeed related to the specific features of the amino acids.

Overall, the data reported show that the interaction of a model protein with the TCC5 monolayer and TCC5–amino acid bilayers yields a class of uniform adsorption processes, providing a very fast and stable immobilization of lysozyme as model protein in a well-defined quantity, owing to the controlled number of covalently bound calix hosting sites. Furthermore, simple considerations based on evaluated lysozyme footprints, for TCC5 monolayers and TCC5–amino acid bilayers, suggest that lysozyme molecules are, respectively, anchored in end-on and slightly tilted end-on orientation. Accordingly, the amino acid/calix bilayers described in this paper may represent, in general, a new and effective class of templating systems, able to build new versatile and smart biomimetic surfaces, capable of the fine-tuning both the number and the orientation of anchored protein molecules.

Supplementary material

The supplementary material for this article can be found at https://doi.org/10.1557/mrc.2018.54

Acknowledgments

G. M. L. Messina acknowledges the financial support by FIRB 2013—Future in Research (MIUR, Rome). C. Bonaccorso acknowledges the University of Catania for a post-doctoral Fellowship. G. Marletta acknowledges the partial financial support from FIR 2014 (University of Catania).

References

1. D.G. Castner and B. D. Ratner: Biomedical surface science: foundations to frontiers. *Surf. Sci.* **500**, 28 (2002).
2. J. J. Gray: The interaction of proteins with solid surfaces. *Curr. Opin. Struct. Biol.* **14**, 110 (2004).
3. N. Tuccitto, N. Giamblanco, A. Licciardello, and G. Marletta: Patterning of lactoferrin using functional SAMs of iron complexes. *Chem. Commun.* **25**, 2621 (2007).
4. B. Kasemo: Biological surface science. *Surf. Sci.* **500**, 656 (2002).
5. C. Satriano, G.M.L. Messina, S. Carnazza, S. Guglielmino, and G. Marletta: Bacterial adhesion onto nanopatterned polymer surfaces. *Mat. Sci. Eng. C* **26**, 942 (2006).
6. M. Manso Silvàn, G.M.L. Messina, I. Montero, C. Satriano, J.P. Garcìa Ruiz, and G. Marletta: Aminofunctionalization and sub-micrometer patterning on silicon through silane doped agarose hydrogels. *J. Mater. Chem.* **19**, 5226 (2009).
7. C. Fotia, G.M.L. Messina, G. Marletta, N. Baldini, and G. Ciapetti: Hyaluronan-based pericellular matrix: substrate electrostatic charges and early cell adhesion events. *Eur. Cell Mater.* **26**, 133 (2013).
8. F. A. Denis, P. Hanarp, D. S. Sutherland, J. Gold, C. Mustin, P. G. Rouxhet, and Y. F. Dufrene: Protein adsorption on model surfaces with controlled nanotopography and chemistry. *Langmuir* **18**, 819 (2002).
9. M. Dettin, A. Zamuner, M. Roso, A. Gloria, G. Iucci, G.M.L. Messina, U. D'Amore, G. Marletta, M. Modesti, I. Castagniulo, and P. Brun: Electrospun scaffolds for osteoblast cells: peptide-induced concentration-dependent improvements of polycaprolactone. *PLoS ONE* **10**(9), e0137505 (2005).
10. M. A. Donovan, Y. Y. Yimer, J. Pfaendtner, E.H.G. Backus, M. Bonn, and T. Weidner: Ultrafast reorientational dynamics of leucine at the air–water interface. *J. Am. Chem. Soc.* **138**, 5226 (2016).
11. P. Roach, D. Farrar, and C. C. Perry: Interpretation of protein adsorption: surface-induced conformational changes. *J. Am. Chem. Soc.* **127**, 8168 (2005).
12. C. F. Wertz and M. M. Santore: Adsorption and reorientation kinetics of lysozyme on hydrophobic surfaces. *Langmuir* **18**, 1190 (2002).
13. P. Brun, M. Scorzeto, S. Vassanelli, I. Castagliuolo, G. Palù, F. Ghezzo, G. M.L. Messina, G. Iucci, V. Battaglia, S. Sivolella, A. Bagno, G. Polzonetti, G. Marletta, and M. Dettin: Mechanisms underlying the attachment and spreading of human osteoblasts: from transient interactions to focal adhesions on vitronectin-grafted bioactive surfaces. *Acta. Biomater.* **9**, 6105 (2013).
14. P. Neri, J. L. Sessler, and M.-X. Wang, eds. *Calixarenes and Beyond* (Springer International Publishing, Cham, 2016).
15. J. Vicens, J. Harrowfield, and L. Baklouti, eds. *Calixarenes in the Nanoworld* (Springer, The Netherlands, 2007).
16. C. Bonaccorso, G. Brancatelli, G. Forte, G. Arena, S. Geremia, D. Sciotto, and C. Sgarlata: Factors driving the self-assembly of water-soluble calix[4]arene and gemini guests: a combined solution, computational and solid-state study. *RSC Adv.* **4**, 53575 (2014).
17. C. Escudero, A. D'Urso, R. Lauceri, C. Bonaccorso, D. Sciotto, S. Di Bella, Z. El-Hachemi, J. Crusats, J.M. Ribò, and R. Purrello: Hierarchical dependence of porphyrin self-aggregation: controlling and exploiting the complexity. *J. Porphyr. Phthalocyanines* **14**, 708 (2010).
18. T. Mecca, G. M. L. Messina, G. Marletta, and F. Cunsolo: Novel pH responsive calix[8]arene hydrogelators: self-organization processes at a nanometric scale. *Chem. Commun.* **49**, 2530 (2002).
19. C. Bonaccorso, G. Brancatelli, F. P. Ballistreri, S. Geremia, A. Pappalardo, G. A. Tomaselli, R. M. Toscano, and D. Sciotto: Novel chiral (salen)Mn(III) complexes containing a calix[4]arene unit in 1,3-alternate conformation

https://doi.org/10.1557/mrc.2018.54 Published online by Cambridge University Press

as catalysts for enantioselective epoxidation reactions of (*Z*)-aryl alkenes. *Dalton Trans.* **43**, 2183 (2014).
20. A.T. Almeida, M.C. Salvadori, and D.F.S. Petri: Enolase adsorption onto hydrophobic and hydrophilic solid substrates. *Langmuir* **18**, 6914 (2002).
21. C. S. Park, H. J. Lee, A. C. Jamison, and T. R. Lee: Robust maleimide-functionalized gold surfaces and nanoparticles generated using custom-designed bidentate adsorbates. *Langmuir* **32**, 7306 (2016).
22. M. I. Béthencourt, L. Srisombat, P. Chinwangso, and T. R. Lee: SAMs on gold derived from the direct adsorption of alkanethioacetates are inferior to those derived from the direct adsorption of alkanethiols. *Langmuir* **25**, 1265 (2009).
23. A. Ulman: Formation and structure of self-assembled monolayers. *Chem. Rev.* **96**, 1533 (1996).
24. A. Feiler, A. Sahlholm, T. Sandberg, and K. D. Caldwell: Adsorption and viscoelastic properties of fractionated mucin (BSM) and bovine serum albumin (BSA) studied with quartz crystal microbalance (QCM-D). *J. Colloid Interface Sci.* **315**, 475 (2007).
25. G. Sauerbrey: Verwendung von Schwingquarzen zur Wägung dünner Schichten und zur Mikrowägung. *Z. Phys.* **55**, 206 (1959).
26. J.-Y. Park, B.-C. Kim, and S.-M. Park: Molecular recognition of protonated polyamines at calix[4]crown-5 self-assembled monolayer modified electrodes by impedance measurements. *Anal. Chem.* **79**, 1890 (2007).
27. M. Rabe, D. Verdes, and S. Seeger: Understanding protein adsorption phenomena at solid surfaces. *Adv. Colloid Interface* **87**, 162 (2011).
28. Z.G. Peng, K. Hidajat, and M.S. Uddin: Selective and sequential adsorption of bovine serum albumin and lysozyme from a binary mixture on nanosized magnetic particles. *J. Colloid Interface Sci.* **11**, 281 (2005).
29. F. Dismer and J. Hubbuch: A novel approach to characterize the binding orientation of lysozyme on ion-exchange resins. *J. Chromatogr. A* **312**, 1149 (2007).
30. K. Kubiak, Z. Adamczyk, and M. Ocweieja: Kinetics of silver nanoparticle deposition at PAH monolayers: reference QCM results. *Langmuir* **31**, 2988 (2015).

https://doi.org/10.1557/mrc.2018.54 Published online by Cambridge University Press